

Short Communication

Electrochemical Studies of Three Disamarium Large Metallofullerenes $\text{Sm}_2@D_2(35)\text{-C}_{88}$, $\text{Sm}_2@C_1(21)\text{-C}_{92}$ and $\text{Sm}_2@D_{3d}(822)\text{-C}_{104}$

Jie Chen, Pei Zhang, Jianfeng Zhao, Hua Yang, and Ziyang Liu*

College of Materials Science and Engineering, China Jiliang University, Hangzhou 310018, China

*E-mail: zyliu@cjl.u.edu.cn

Received: 16 March 2015 / Accepted: 3 May 2015 / Published: 4 June 2016

We isolated and purified three disamarium metallofullerenes of known structure, $\text{Sm}_2@D_2(35)\text{-C}_{88}$, $\text{Sm}_2@C_1(21)\text{-C}_{92}$ and $\text{Sm}_2@D_{3d}(822)\text{-C}_{104}$, by the reported method. Importantly, we characterized these three di-samarium metallofullerenes by cyclic voltammetry and differential pulse voltammetry, which is the first report of electrochemical studies of di-metallofullerenes containing divalent metal atoms. Their oxidation reactions are observed at a maximum positive potential compared with other endohedral metallofullerenes (EMFs), which, other than those of mono-samarium metallofullerenes, have never been reported. The electrochemical studies of these three compounds show much weaker electron-donating capacity and stronger electron-accepting capacity compared with the corresponding Sm-EMFs, fullerenes, or cluster-metallofullerenes. Interestingly, further analysis shows that normal-metallofullerenes present narrower electrochemical potential gaps than cluster-metallofullerenes, which might be attributed to their stronger interaction between the inner metal ions and the carbon cage.

Keywords: endohedral metallofullerene, di-samarium, electrochemistry, cyclic voltammetry (CV), differential pulse voltammetry (DPV)

1. INTRODUCTION

Since the 1990s, endohedral metallofullerenes (EMFs), which consist of a closed carbon cage with one to three metal atoms or metal clusters encaged inside, have been paid much attention by scientists worldwide. [1, 2] It has been found that EMFs exhibit many novel properties, which are the result of changing the species, nature and number of the trapped metal atoms. Therefore, endohedral

metallofullerenes have a variety of potential applications, such as magnetic resonance imaging, [3, 4] X-ray imaging, [5] and photovoltaic conversion. [6]

Generally, the soot produced in the routine arc discharging condition contains several kinds of EMFs, including normal mono-, di-, and tri-metal endohedrals ($M@C_{2n}$, $M_2@C_{2n}$, $M_3@C_{2n}$) and metal carbide cluster-endohedrals ($M_2C_2@C_{2n}$), some of which have been structurally identified by magnetic nuclear resonance (NMR) or single-crystal diffraction. [7, 8] Well-characterized examples of the mono-metal EMF class include $La@C_{2v}(9)-C_{82}$ [9] and $Yb@C_{80, 82, 84}$. [10] Examples of the metal carbide cluster-endohedral class include $Sc_2(\mu-C_2)@C_{68}$, [11] $Sc_2(\mu-C_2)@C_{2v}(5)-C_{80}$ [12] and the three isomers of $M_2(\mu-C_2)@C_{82}$ ($M = Sc, Y$), [13] $Sc_2(\mu-C_2)@D_{2d}-C_{84}$, [14] and $Gd_2(\mu-C_2)@D_3(85)-C_{92}$. [15] Examples of the di-metal class include $Er_2@C_s(6)-C_{82}$, [16] $Er_2@C_{3v}(8)-C_{82}$, [17] $La_2@I_h-C_{80}$, [18] $M_2@D_{3h}-C_{78}$ ($M = Ce$, [19] La [20]) and the non-IPR $La_2@C_2(10611)-C_{72}$. [21] Recently, Yang and coworkers identified four large disamarium EMFs in the form of $Sm_2@C_{2n}(n=44-46, 52)$ by an X-ray crystallographic method using synchrotron radiation.

While the structures of above EMFs have been extensively characterized, there have been few reports on investigations of their electrochemistry, especially the large endohedral metallofullerenes. It is well known that electrochemical investigation is very important for EMFs as it can provide much information on their electronic structures and redox properties. Recently, Liu and coworkers performed electrochemical research on a series of monosamarium EMFs ranging from $Sm@C_{74}$ to $Sm@C_{90}$. Some metal cluster endohedral metallofullerenes such as $Sc_2C_2@C_s(10528)-C_{72}$, [22] $Sc_2C_2@C_{2v}(5)-C_{80}$, [23] $Sc_2C_2@C_{82}(III)$, [24] $Sc_2S@C_{82}(C_s:6)$, [25] $Y_3N@D_2(35)-C_{88}$ [26] and $La_3N@C_{88}$ [27] have recently been characterized by cyclic voltammetry (CV) and differential pulse voltammetry (DPV). It is thought that there is a great difference between normal metal endohedrals and metal carbide cluster ones in both their geometric structures and physical chemistry properties. With regard to the electrochemical study of disamarium endohedral fullerenes with two divalent samarium ions encaged, $(M_2)^{4+}@C_{2n}^{4-}$, the CV and DPV measurements are missing. Herein, we report a systematic study of the electrochemistry of high disamarium metallofullerenes including $Sm_2@D_2(35)-C_{88}$, $Sm_2@D_3(85)-C_{92}$, and $Sm_2@D_{3d}(822)-C_{104}$. Based on the experimental data, the influence of the trapped metal atoms and of the cage's size on the electronic properties of endohedral fullerenes is discussed.

2. EXPERIMENTAL SECTION

The CVs and DPVs were determined using a CHI-610D electrochemical analyser. Electrochemistry experiments were carried out in o-DCB (anhydrous, 99%, Aladdin), with TBAPF₆ (0.5 M) as the supporting electrolyte. All the tests were conducted in a small electrolytic cell with a Pt wire, a Pt wire and a SCE as the working, counter and reference electrodes, respectively. Tetrabutylammonium hexafluorophosphate (TBAPF₆) was re-crystallized from high-purity ethanol and dried in vacuum before use. The compounds were purified using a Waters HPLC device. The electrochemical cell was deoxidized with high-purity He for 15 min before each test. Cyclic voltammograms were measured at a scan rate of 50 mV/s, and differential pulse voltammograms were recorded by using a pulse height, width and period of 50 mV, 50 ms and 500 ms, respectively.

Ferrocene (Fc) was added to the solution at the end of each measurement as an internal potential standard.

3. RESULTS AND DISCUSSION

According to the method reported by Yang and co-workers, we isolated and purified three large disamarium metallofullerenes, which gave similar UV/vis/NIR spectra to known structures identified by the X-ray crystallographic method, $\text{Sm}_2@D_2(35)\text{-C}_{88}$, $\text{Sm}_2@C_1(21)\text{-C}_{92}$ and $\text{Sm}_2@D_{3d}(822)\text{-C}_{104}$, respectively.[28, 29] Cyclic voltammetry and differential pulse voltammetry, two valuable electrochemical techniques to analyse the electronic structures of compounds, have been performed on these three disamarium metallofullerenes. Figure 1 shows the CVs and DPVs of the as-synthesized $\text{Sm}_2@D_2(35)\text{-C}_{88}$ and $\text{Sm}_2@D_3(85)\text{-C}_{92}$. As can be seen, the CVs of $\text{Sm}_2@D_2(35)\text{-C}_{88}$ and $\text{Sm}_2@D_3(85)\text{-C}_{92}$ at a scan rate of $50 \text{ mV}\cdot\text{s}^{-1}$ show three reversible reduction peaks and one oxidation peak, but there are clearly two reversible reduction peaks and one oxidation peak for $\text{Sm}_2@D_{3d}(822)\text{-C}_{104}$ (Figure 1A). The reversible redox peaks of each compound have approximately equal peak heights, which show that they can be ascribed to a one-electron process. The first reduction potentials of $\text{Sm}_2@D_2(35)\text{-C}_{88}$, $\text{Sm}_2@C_1(21)\text{-C}_{92}$ and $\text{Sm}_2@D_{3d}(822)\text{-C}_{104}$ present an increasing trend, but the second reduction potentials no longer have this tendency; rather, that of $\text{Sm}_2@C_1(21)\text{-C}_{92}$ is slightly higher. $\text{Sm}_2@D_2(35)\text{-C}_{88}$ and $\text{Sm}_2@C_1(21)\text{-C}_{92}$ show similar third reduction potentials around -1.0 V , while $\text{Sm}_2@D_{3d}(822)\text{-C}_{104}$ lacks a corresponding peak.

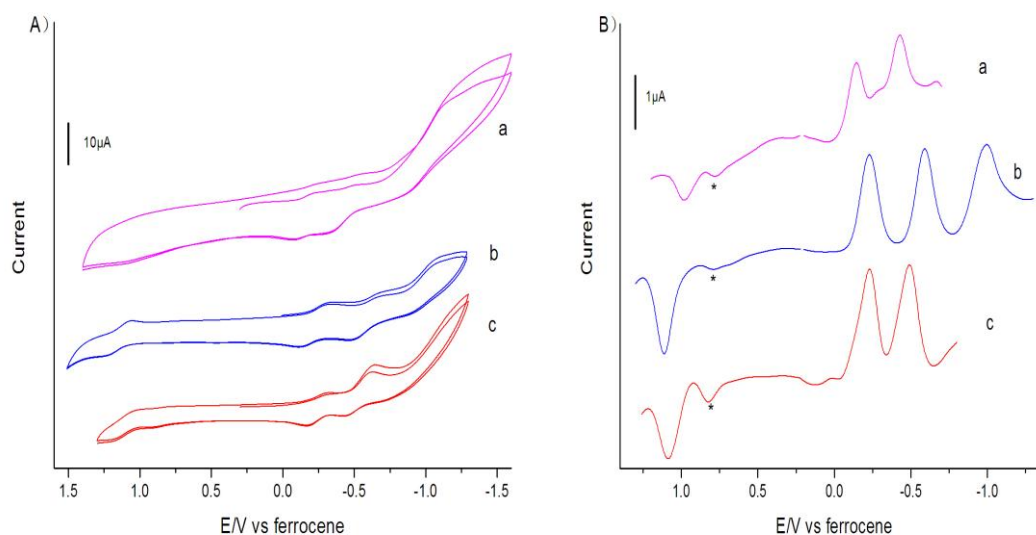


Figure 1. Cyclic (A) and differential pulse (B) voltammograms of $\text{Sm}_2@D_2(35)\text{-C}_{88}$ (a), $\text{Sm}_2@C_1(21)\text{-C}_{92}$ (b) and $\text{Sm}_2@D_{3d}(822)\text{-C}_{104}$ (c) in o-DCB containing 0.5 M TBAPF₆ with ferrocene as the internal standard at a scan rate of 50 mV s^{-1} . The asterisk-marked peak is caused by an impurity.

It is interesting that the oxidation potentials of these disamarium metallofullerenes are higher than those of any other normal metallofullerene or endohedral cluster-metallofullerene electrochemically studied, including carbide-cluster metallofullerenes and TNT metallofullerenes. While notable, EMFs containing a single divalent metal atom have never been reported to be observed. Meanwhile, Xu early reported two oxidation steps of $\text{Sm}_3@I_h\text{-C}_{80}$ at the potentials of 0.30 V and 0.78 V, which are much lower than those of our disamarium EMFs. [30]

The redox potentials and electrochemical band gaps of the three disamarium metallofullerenes estimated by CV and DPV are summarized in Table 1. As can be observed, when comparing the first reduction potentials of these three disamarium endohedrals with those of monosamarium metallofullerenes at the same experimental conditions, the first reduction potentials of $\text{Sm}_2@C_{I(21)\text{-}C_{92}}$ (-0.25 V) are all more positive than those of $\text{Sm}@C_{92(\text{I})}$ (-0.61 V) and $\text{Sm}@C_{92(\text{II})}$ (-0.40 V). Upon comparing the data between $\text{Sm}_2@D_2(35)\text{-}C_{88}$ (-0.14 V) and the corresponding mono-samarium EMF, $\text{Sm}@C_{88}$, it is unfortunate that there were no corresponding electrochemical data from Liu's article (Liu J) due to the extremely low yield. Certainly, the CV and DVP data of $\text{Sm}_2@D_{3d}(822)\text{-}C_{104}$ could not be matched because $\text{Sm}_2@D_{3d}(822)\text{-}C_{104}$ is the largest structure-identified metallofullerene in both the empty and endohedral fullerenes. Additionally, the first reduction potentials of these three disamarium endohedral metallofullerenes are also higher than those of other $\text{Sm}@C_{2n}(2n=74\sim 96)$ [31] besides $\text{Sm}@C_{2v}\text{-}C_{82}$. It can be expected that these disamarium endohedral metallofullerenes become better electron acceptors due to the participation of the second Sm atoms.

It is known that the first reduction potentials of C_{60} , C_{70} , C_{76} , C_{78} , and C_{84} present a decreasing tendency. [32] However, there is no linear relation to the size of cage for monosamarium EMFs, which was explained by the symmetrical structures of the carbon cages that have a great influence on their electronic properties. [29] However, the first reduction potentials of our three samples gradually increase from -0.14 to -0.25 with growth in size of the carbon cages. The frontier orbital energy of C_{2n} changes as electrons transfer from trapped metal atoms to carbon cages. In addition, the electron number of the π system increases with the cage size.

Table 1. Redox potentials of disamarium metallofullerenes vs Fc/Fc^+ (in volts) ^[a]

Compound		$E_{1/2}^{\text{ox}}$	$E_{1/2}^{\text{red1}}$	$E_{1/2}^{\text{red2}}$	$E_{1/2}^{\text{red3}}$	$\Delta E_{\text{gap}}^{\text{[b]}}$
$\text{Sm}_2@D_2(35)\text{-}C_{88}$	CV	1.01	-0.14	-0.45	-1.01	1.25
	DPV	0.98	-0.15	-0.43	—	1.23
$\text{Sm}_2@C_{I(21)\text{-}C_{92}}$	CV	1.12	-0.22	-0.59	-0.97	1.34
	DPV	1.10	-0.22	-0.58	-0.98	1.32
$\text{Sm}_2@D_{3d}(822)\text{-}C_{104}$	CV	1.12	-0.25	-0.53	—	1.37
	DPV	1.10	-0.23	-0.52	—	1.33

[a] The CVs were measured in o-DCB containing 0.5 M TBAPF₆; scan rate: 50 mV/s. DPVs used a pulse amplitude: 50 mV; pulse width: 50 ms; and pulse period: 500 ms. [b] $\Delta E_{\text{gap}} = E_{1/2}^{\text{ox1}} - E_{1/2}^{\text{red1}}$.

Thus, it can be inferred that the influence of transferred electrons is weaker for larger cages, as described previously by Liu and Gu. [31] By this token, the weaker influence causes the electronic properties of dimetallofullerenes based on larger cages to be more similar to those of

the corresponding hollow fullerenes that used to have a relatively high reduction potential. Therefore, the higher Sm-dimetallofullerenes show a more negative reduction. With respect to the second reduction potentials, that of $\text{Sm}_2@D_2(35)\text{-C}_{88}$ is still the lowest, but the potential of $\text{Sm}_2@D_3(85)\text{-C}_{92}$ is higher than that of $\text{Sm}_2@D_{3d}(822)\text{-C}_{104}$, which might be due to the symmetrical structure of the carbon cage. In addition, the gaps between the first and second reduction potentials of $\text{Sm}_2@D_2(35)\text{-C}_{88}$, $\text{Sm}_2@D_3(85)\text{-C}_{92}$ and $\text{Sm}_2@D_{3d}(822)\text{-C}_{104}$ are 0.31 V, 0.37 V and 0.28 V, respectively. These gaps are relatively narrow, which indicates that the two electrons participating in the front two reductions are accepted by the same molecular orbital. That is to say, the HOMOs of these three dimetallofullerenes are filled with two electrons.

The oxidation reactions of these three dimetallofullerenes were also characterized by CV and DPV in our work. However, those of endohedral fullerenes containing a single divalent metal atom were never observed. It seems that the more divalent metal atoms are entrapped in an endohedral fullerene, the more easily they can be oxidized, and thus, the undetected oxidation potentials of the Sm-EMFs might be too high for the observable window of the solvent used. In addition, the electrochemical band gaps (ΔE_{gap}) of these three disamarium EMFs are 1.25 V, 1.34 V and 1.37 V, respectively, which presents a gradual increase with the growth of the.

The electrochemical potential gap, computed molecular orbital and spectral band gap of $\text{Sm}_2@D_{3d}(822)\text{-C}_{104}$ are illustrated in table 2. The very high first oxidation potential and the relatively high first reduction potential of $\text{Sm}_2@D_{3d}(822)\text{-C}_{104}$ cause it to have a larger electrochemical potential gap than analogous gaps found for $\text{Sm}_2@D_2(35)\text{-C}_{88}$ and $\text{Sm}_2@C_1(21)\text{-C}_{92}$. Meanwhile, this large ΔE_{gap} is in good agreement with the DFT-predicted wide HOMO-LUMO gap and the reported spectral onset. [29] As is known, a wide energy gap implies a good dynamic stability, which has a significant influence on the production yield of endohedral metallofullerenes. Experimentally, the abundance of $\text{Sm}_2@D_{3d}(822)\text{-C}_{104}$ is dominant with the range of carbon cages from C_{98} to C_{108} , which is a reflection of its excellent dynamic stability, as supported by our electrochemical measurement, early spectrometric assay, and DFT computations. It is serendipitous that our group that first isolated $\text{Sm}_2@D_{3d}(822)\text{-C}_{104}$, which contains such a large cage, early in 2009. [29] As the mass spectrum shows, 104 seems to be a magic number for disamarium metallofullerenes due to the overwhelming yield of di-Sm EMFs based on C_{104} (see supporting information of ref 6).

Table 2. Redox potentials^[a], HOMO-LUMO levels^[b] and band gaps^[c] of $\text{Sm}_2@D_{3d}(822)\text{-C}_{104}$

Compound	Electrochemistry			DFT-calculation			Spectrum	
	$E_{1/2}^{\text{ox1}}$ [V]	$E_{1/2}^{\text{red1}}$ [V]	ΔE_{gap} [V]	HOMO [eV]	LUMO [eV]	H-L gap[eV] ^[c]	Onset ^[d] [nm]	Band gap ^[d] [eV]
$\text{Sm}_2@D_{3d}(822)\text{-C}_{104}$	1.12	-0.25	1.37	-5.99	-4.30	1.69	890	1.39

[a] Redox potentials are half-cell potentials, values are relative to the ferrocene/ferrocenium couple. [b] HOMO-LUMO data taken from ref 6. [c] H-L gap = LUMO-HOMO. [d] Onset date taken from ref 6, band gap is calculated from the spectral onset (band gap [eV] \approx 1240/onset [nm]).

The redox potentials of several endohedral fullerenes obtained from CV are summarized in Table 3. Compared with those of other species that have been reported to have the same cage, the first oxidation potential of $\text{Sm}_2@D_2(35)\text{-C}_{88}$ is much higher than that of $\text{Y}_3\text{N}@D_2(35)\text{-C}_{88}$, [26] indicating a very weak electron-donating property. Our disamarium EMFs have a very high oxidative resistance, as no oxidation was detected upon exposure to the open air for a long time. Exceptionally, $\text{La}@C_{82}$ has less stability under air, with an extremely low oxidation potential (0.07 V), as is known. [33] The first reduction potential of $\text{Sm}_2@D_2(35)\text{-C}_{88}$ is much lower than that of $\text{Y}_3\text{N}@D_2(35)\text{-C}_{88}$, suggesting a strong electron-accepting ability. Clearly, $\text{Sm}_2@D_2(35)\text{-C}_{88}$ and $\text{Sm}_2@C_{71}(21)\text{-C}_{92}$ have similar electronic properties. This strong electron-accepting ability results in a complementarity of surface potentials between EMFs and $[\text{Ni}(\text{OEP})]$ (OEP = octaethylporphyrin), which displays a negative potential. [34] Thus, their cocrystals with $[\text{Ni}(\text{OEP})]$ are comparatively easy to obtain. In addition, compared with other endohedral fullerenes with clusters in the 4+ oxidation state, like $\text{Sc}_2\text{C}_2@C_s(10528)\text{-C}_{72}$ ($E^{\text{ox}1} = 0.41$ V, $E^{\text{red}1} = -1.19$ V) [22] or $\text{Sc}_2\text{S}@C_{82}(C_s:6)$ ($E^{\text{ox}1} = 0.45$ V, $E^{\text{red}1} = -1.01$ V), [25] these three Sm-endohedral dimetallofullerenes also show a much weaker electron-donating capacity and stronger electron-accepting capacity.

Table 3. Redox potentials^[a] and ΔE_{gap} s of endohedral fullerenes

Ref.	Compound	$E_{1/2}^{\text{ox}1}$ [V]	$E_{1/2}^{\text{red}1}$ [V]	ΔE_{gap} ^[b] [V]	Onset[eV]
this work	$\text{Sm}_2@D_2(35)\text{-C}_{88}$	1.01	-0.14	1.25	0.85
26	$\text{Y}_3\text{N}@D_2(35)\text{-C}_{88}$	0.03	-1.43	1.46	1.49
27	$\text{La}_3\text{N}@C_{88}$	0.21	-1.34	1.57	0.87
25	$\text{Sc}_2\text{S}@C_{82}(C_s:6)$	0.45	-1.01	1.46	0.92
24	$\text{Sc}_2\text{C}_2@C_{82}(\text{III})$	0.53	-0.94	1.47	—
22	$\text{Sc}_2\text{C}_2@C_s(10528)\text{-C}_{72}$	0.41	-1.19	1.60	—
30, 31	$\text{Sm}@C_{71}(42)\text{-C}_{92}$	—	-0.61	—	0.93
35	$\text{Sm}_3@I_h\text{-C}_{80}$	0.30	-0.83	1.13	1.38
36	$\text{Ce}_2@C_{80}$	0.57	-0.39	0.96	—
33	$\text{La}@C_{82}(C_{2v})$	0.07	-0.42	0.49	0.75
31	$\text{Sm}@C_{82}(C_{2v})$	—	-0.22	—	0.78

[a] Redox potentials are half-cell potentials, values are relative to the ferrocene/ferrocenium couple. [b] $\Delta E_{\text{gap}} = E_{1/2}^{\text{ox}1} - E_{1/2}^{\text{red}1}$. [c] Onset[eV] is calculated from the spectral onset (Onset[eV] \approx 1240/onset [nm]).

Table 3 shows the ΔE_{gap} s of several endohedral fullerenes. It can be observed that normal-metallofullerenes, $\text{M}_m@C_{2n}$ ($m=1, 2, 3$), all show narrower electrochemical potential gaps than endohedral cluster-metallofullerenes $\text{M}_m\text{X}_l@C_{2n}$ ($m=2, 3; l=1, 2$). As discussed above, one can understand this electrochemical phenomenon by taking the influence between the inner metal ions and the carbon cage into consideration. The significant differences might be attributed to the different effective strengths of their metal-cage bonds. The shortest distances between the encaged metal ions

and the carbon atoms of the cage for the most populated sites are 2.484(7) Å and 2.50 Å, respectively in $\text{Gd}_2\text{C}_2@D_3(85)\text{-C}_{92}$ and $\text{Sm}_2@C_1(21)\text{-C}_{92}$. [15, 28] Taking the difference between the ionic radii 0.28 Å of Sm^{2+} (1.22 Å) and Gd^{3+} (0.94 Å) into consideration, the interaction of the Sm-cage is more favourable than that of the Gd-cage. [37] Similarly, by considering the ionic radii of Tb^{3+} (0.92 Å), Sc^{3+} (0.75 Å) and Er^{3+} (0.89 Å), it can be found that the interactions of the Sm-cages in $\text{Sm}_2@D_2(35)\text{-C}_{88}$ ($d_{\text{Sm-C}}=2.51$ Å)^[28] and $\text{Sm}_3@I_h\text{-C}_{80}$ ($d_{\text{Sm-C}}=2.40$ Å)^[35] and the Er-cage in $\text{Er}_2@C_{3v}(82:8)\text{-C}_{82}$ ($d_{\text{Er-C}}=2.29$ Å)^[17] are distinctly stronger than those of the Tb-cage and Sc-cage in $\text{Tb}_3\text{N}@C_{88}$ ($d_{\text{Tb-C}}=2.333$ Å)^[38] and $\text{Sc}_2\text{C}_2@C_{82}(C_{3v}:8)$ ($d_{\text{Sc-C}}=2.29$ Å)^[39], respectively, when the cage sizes are similar. These geometric differences indicate that the metal ions in normal metallofullerenes are more constrained by the carbon cage than those in cluster-metallofullerenes. This result must influence the interactions between the cage and the encaged metal ions and, thus, their electrochemical properties. Therefore, endohedral metallofullerenes can be divided into two groups, normal-metallofullerenes and cluster-metallofullerenes, based on their different energy gaps. $\text{M}_2@C_{2n}$, along with $\text{M}@C_{2n}$ and $\text{M}_3@C_{2n}$, as normal-metallofullerenes, have stronger interactions between the metal ions and the cage than cluster-metallofullerenes, whose metal ions are attracted by the inner nonmetallic attractor. Consequently, the electron density of their cage overlaps with the inner metal ions and exhibits narrower electrochemical potential gaps. Moreover, the ranges of Sm-C distances in $\text{Sm}_2@D_2(35)\text{-C}_{88}$, $\text{Sm}_2@C_1(21)\text{-C}_{92}$ and $\text{Sm}_2@D_{3d}(822)\text{-C}_{104}$ ^[28, 29] are 2.51-2.66 Å, 2.50-2.77 Å and 2.52-2.72 Å, respectively. The average distances of these three disamarium metallofullerenes gradually increase with the increasing cage size, but that of $\text{Sm}_2@C_1(21)\text{-C}_{92}$ is fairly close to $\text{Sm}_2@D_{3d}(822)\text{-C}_{104}$. These results are also consistent with their observed electrochemical potential gaps.

4. CONCLUSIONS

Three disamarium metallofullerenes, $\text{Sm}_2@D_2(35)\text{-C}_{88}$, $\text{Sm}_2@C_1(21)\text{-C}_{92}$ and $\text{Sm}_2@D_{3d}(822)\text{-C}_{104}$, are isolated and purified by reported methods. Their electronic properties are studied based on information from CV and DPV. As far as we know, this is the first report of the electrochemical studies of a dimetal endohedral-fullerene as $(\text{M}_2)^{4+}@(\text{C}_{2n})^4$. Among them, $\text{Sm}_2@D_{3d}(822)\text{-C}_{104}$ is the largest endohedral-metallofullerene characterized by electrochemical methods until now.

The electronic properties of these three disamarium metallofullerenes are similar. Their first reduction potentials show an increasing trend with the size of the carbon cage. The oxidation processes of disamarium metallofullerenes were carried out by CV and DPV until reaching significant positive potentials. In contrast, those of monosamarium metallofullerenes have never been reported. Compared with the corresponding mono-samarium EMFs and endohedral cluster-metallofullerenes, these three disamarium EMFs act as better electron acceptors and worse electron donators. Furthermore, the demonstrated electrochemical potential gaps of the endohedral metallofullerenes confirm that the species of the encapsulated cluster has a significant effect on the molecular stability. It is agreed that normal metallofullerenes have shorter effective metal-cage bond lengths than cluster-metallofullerenes, thus leading to the stronger interactions between their metal ions and the carbon cage, which results in their narrower electrochemical potential gaps.

ACKNOWLEDGEMENTS

The authors thank the National Natural Science Foundation of China [21271162, 11274283, 11179039] and the Zhejiang International Science and Technology Cooperation Project [2013C24017] for their financial support.

References

1. Y. Chai, T. Guo, C. Jin, R. E. Haufler, L. P. F. Chibante, J. Fure, L. H. Wang, J. M. Alford, R. E. Smally, *J. Phys. Chem.* 95(1991)7564-7568.
2. H. Shinohara, *Rep. Prog. Phys.* 63(2000)843.
3. M. Mikawa, H. Kato, M. Okumura, M. Narazaki, Y. Kanazawa, N. Miwa, H. Shinohara, *Bioconjugate Chem.* 12(2001)510-514.
4. R. D. Bolskar, A. F. Benedetto, L. O. Husebo, R. E. Price, E. F. Jackson, S. Wallace, L. J. Wilson, J. M. Alford, *J. Am. Chem. Soc.* 125(2003)5471.
5. E. B. Iezzi, J. C. Duchamp, K. R. Fletcher, T. E. Glass, H. C. Dorn, *Nano Lett.* 2(2002)1187-1190.
6. R. B. Ross, C. M. Cardona, D. M. Guldi, S. G. Sankaranarayanan, M. O. Reese, N. Kopidakis, J. Peet, B. Walker, G. C. Bazan, E. Van Keuren, B. C. Holloway, M. Drees, *Nature Materials*, 8(3)(2009)208-212.
7. Y. Yamazaki, K. Nakajima, T. Wakahara, T. Tsuchiya, M. O. Ishitsuka, Y. Maeda, T. Akasaka, M. Waelchli, N. Mizorogi, S. Nagase, *Angew. Chem. Int. Ed.* 47(2008)7905-7908.
8. Y. Che, H. Yang, Z. Wang, H. Jin, Z. Liu, C. Lu, T. Zuo, H. Dorn, C. M. Beavers, M. M. Olmstead, A. L. Balch, *Inorg. Chem.* 48(2009)6004.
9. X. Lu, H. Nikawa, T. Tsuchiya, T. Akasaka, M. Toki, H. Sawa, Mizorogi, N. S. Nagase, *Angew. Chem.*, 122(2010)604-607, *Angew. Chem. Int. Ed.* 49(2010)594-597.
10. X. Lu, Z. Slanina, T. Akasaka, T. Tsuchiya, N. Mizorogi, S. Nagase, *J. Am. Chem. Soc.* 132(2010)5896-5905.
11. Z. Q. Shi, X. Wu, C. R. Wang, X. Lu, H. Shinohara, *Angew. Chem., Int. Ed.* 45(2006)2107-2111.
12. H. Kurihara, X. Lu, Y. Iiduka, N. Mizorogi, Z. Slanina, T. Tsuchiya, T. Akasaka, S. J. Nagase, *Am. Chem. Soc.* 133(2011)2382-2385.
13. T. Inoue, T. Tomiyama, T. Sugai, T. Okazaki, T. Suematsu, N. Fujii, H. Utsumi, K. Nojima, H. J. Shinohara, *Phys. Chem. B.* 108(2004)7573-7579.
14. M. Mikawa, H. Kato, M. Okumura, M. Narazaki, Y. Kanazawa, N. Miwa, H. Shinohara, *Bioconjugate Chem.* 12(2001)510-514.
15. H. Yang, C. X. Lu, Z. Y. Liu, H. X. Jin, Y. L. Che, M. M. Olmstead, A. L. Balch, *J. Am. Chem. Soc.* 130(2008)17296-17300.
16. M. M. Olmstead, A. de Bettencourt-Dias, S. Stevenson, H. C. Dorn, A. L. Balch, *J. Am. Chem. Soc.* 124(2002)4172-4173.
17. M. M. Olmstead, H. M. Lee, S. Stevenson, H. C. Dorn, A. L. Balch, *Chem. Commun.* (2002)2688-2689.
18. T. Akasaka, S. Nagase, K. Kobayashi, M. Walchli, K. Yamamoto, H. Funasaka, M. Kako, T. Hoshino, T. Erata, *Angew. Chem. Int. Ed.* 36(1997)1643-1645.
19. B. P. Cao, T. Wakahara, T. Tsuchiya, M. Kondo, Y. Maeda, G. M. A. Rahman, T. Akasaka, K. Kobayashi, S. Nagase, K. J. Yamamoto, *Am. Chem. Soc.* 126(2004)9164-9165.
20. B. Cao, H. Nikawa, T. Nakahodo, T. Tsuchiya, Y. Maeda, T. Akasaka, H. Sawa, Z. Slanina, N. Mizorogi, N. J. Nagase, *Am. Chem. Soc.* 130(2008) 983-989.
21. X. Lu, H. Nikawa, T. Tsuchiya, Y. Maeda, M. O. Ishitsuka, T. Akasaka, M. Toki, H. Sawa, Z. Slanina, N. Mizorogi, S. Nagase, *Angew. Chem. Int. Ed.* 47(2008)8642-8645.
22. Y. Feng, T. Wang, J. Wu, L. Feng, J. Xiang, Y. Ma, Z. Zhang, L. Jiang, C. Shu, C. Wang, *Nanoscale.* 5(2013)6704-6707.

23. H. Kurihara, X. Lu, Y. Iiduka, H. Nikawa, N. Mizorogi, Z. Slanina, T. Tsuchiya, S. Nagase, and T. Akasaka, *J. Am. Chem. Soc.* 134(2012)3139–3144.
24. Y. Iiduka, T. Wakahara, K. Nakajima, T. Nakahodo, T. Tsuchiya, Y. Maeda, T. Akasaka, K. Yoza, M. T. H. Liu, N. Mizorogi, and S. Nagase, *Angew. Chem. Int. Ed.* 46(2007)5562–5564.
25. N. Chen, M. N. Chaur, C. Moore, J. R. Pinzon, R. Valencia, A. R. Fortea, J. M. P. L. Echegoyen, *Chem. Commun.*, 46(2010)4818–4820.
26. W. Fu, J. Zhang, H. Champion, T. Fuhrer, H. Azuremendi, T. Zuo, J. Zhang, K. Harich and H. C. Dorn, *Inorg. Chem.* 50(2011)4256–4259.
27. M. M. Olmstead, H. M. Lee, S. Stevenson, H. C. Dorn and A. L. Balch, *Chem. Commun.* (2002)2688–2689.
28. H. Yang, H. Jin, B. Hong, Z. Liu, C. M. Beavers, H. Zhen, Z. Wang, Brandon Q. Mercado, Marilyn M. Olmstead, and Alan L. Balch, *J. Am. Chem. Soc.* 133(2011)16911–16919.
29. Brandon Q. Mercado, A. Jiang, H. Yang, Z. Wang, H. Jin, Z. Liu, Marilyn M. Olmstead, and Alan L. Balch, *Angew. Chem. Int. Ed.* 48(2009)9114–9116.
30. H. Jin, H. Yang, M. Yu, Z. Liu, C. M. Beavers, M. M. Olmstead and A. L. Balch, *J. Am. Chem. Soc.* 314(2012)10933–10941.
31. J. Liu, Z. Shi, and Z. Gu, *Chem. Asian J.* 4(2009)1703–1711.
32. P. Boulas, M. T. Jones, K. Kadish, R. Ruoff, D. C. Lorents, R. Mal-hotra, D. S. *Tse in Recent Advances in the Chemistry and Physics of Fullerenes*, Vol. 1, (Eds: K. Kadish, R. Ruoff), San Francisco, USA, (1994)1007.
33. T. Suzuki, Y. Maruyama, T. Kato, K. Kikuchi, Y. J. Achiba, *Am. Chem. Soc.* 115(1993)11006.
34. H. Yang, Z. Wang, H. Jin, B. Hong, Z. Liu, C. M. Beavers, M. M. Olmstead, A. L. Balch, *Inorg. Chem.* 52(2013)1275–1284.
35. W. Xu, L. Feng, M. Calvaresi, J. Liu, Y. Liu, B. Niu, Z. Shi, Y. Lian, and F. Zerbetto, *J. Am. Chem. Soc.* 135(2013)4187–4190.
36. M. Yamada, T. Nakahodo, T. Wakahara, T. Tsuchiya, Y. Maeda, T. Akasaka, M. Kako, K. Yoza, E. Horn, N. Mizorogi, K. Kobayashi, S. J. Nagase, *Am. Chem. Soc.* 127(2005)14570–14571.
37. *CRC Handbook of Chemistry and Physics*, 81sted. (Ed.: D. R. Lide), CRC, New York City, (2000).
38. T. Zuo, C. M. Beavers, J. C. Duchamp, A. Campbell, H. C. Dorn, M. M. Olmstead and Alan L. Balch, *J. Am. Chem. Soc.* 129(2007)2035–2043.
39. R. Valencia, A. Rodríguez-Fortea, J. M. Poblet, *J. Phys. Chem. A* 112(2008)4550–4555.